surfaces

MDPI

Article

Relationship between Surface Properties and Fiber Network Parameters of Eucalyptus Kraft Pulps and Their Absorption Capacity

Catarina A. Azevedo [1], Sofia M. C. Rebola [2], Eddy M. Domingues [1,†], Filipe M. L. Figueiredo [1] and Dmitry V. Evtuguin [1,*]

1 CICECO, Department of Chemistry, University of Aveiro, Campus Universitario de Santiago, 3810-193 Aveiro, Portugal; catarinaazevedo@ua.pt (C.A.A.); eddy@ua.pt (E.M.D.); lebre@ua.pt (F.M.L.F.)
2 Celulose Beira Industrial (CELBI) S. A., Leirosa, 3081-853 Figueira da Foz, Portugal; sofia.rebola@altri.pt
* Correspondence: dmitrye@ua.pt
† Present address: TEMA, Department of Mechanical Engineering, University of Aveiro, Campus Universitario de Santiago, 3810-193 Aveiro, Portugal.

Received: 31 May 2020; Accepted: 19 June 2020; Published: 30 June 2020

Abstract: Water absorption capacity is a key characteristic of cellulosic pulps used for different commodities. This property is influenced by the affinity of the pulp fiber surface with water, chemical composition of the pulp, morphology, and organization of fibers in the network. In this study, surface properties of six industrial *Eucalyptus* bleached kraft pulps (fluff pulps) dry-defiberized in a Hammermill, which were obtained by wood pulping and pulp bleaching under different production conditions, were studied while employing dynamic water vapor sorption and contact angles measurements. The absorption properties of air-laid pulp pads were analyzed following the absorbency testing procedure and the relationship between these properties and pulp's chemical composition and fiber network structure were assessed by multivariate analysis. The results showed that the accessibility of the fiber surface is related to the reduction of the contact angles, but, at the same time, to the longer absorption time and less absorption capacity of the fiber network. Therefore, the absorption properties of the pulps are not necessarily directly related to their surface properties. Indeed, absorptivity is related to the surface chemical composition, fiber morphology, and fiber network structure. Thus, surface carboxylic groups promote total water uptake, resulting in better absorption capacity. Greater fiber coarseness and deformations (curl and kink) provide a less wettable surface, but a more porous network with higher specific volume, resulting in more absorbent air-laid formulations.

Keywords: fluff pulp; absorption capacity; sorption isotherms; contact angles; surface wettability; principal component analysis

1. Introduction

Besides for papermaking, wood pulp has been used in absorbent products for many years, being part of common society's goods [1]. Non-paper application of dry-defiberized cellulosic pulps (fluff pulps) includes, but is not limited to, diapers, female hygiene products, air-laid absorbent toweling, surgical pence, and adult incontinence. Capacity expansions and new capacity start-ups are expected to grow in the fluff pulp sector for the next 2–3 years, mainly due to the rising of baby diapers market [2]. Recent interest in fluffy cellulosic materials is related to the low surface stability of SARS-CoV-2 on its surfaces, when compared to common steel and plastic materials [3]. Some strains of coronavirus only live for a few minutes/hours in cellulosic networks that, being a porous absorbable material, cause

the virus to be stuck and dry. This fact opens new horizons in the manufacture of a wide range of disposable means of cleaning and protection using fluff pulps.

Fluff pulp is made of softwood or hardwood cellulosic pulps, which are produced by kraft or sulphite pulping [4]. The aim is to produce a pulp that can be well defiberized when dry [1,4]. Fluff pulps that are made of softwood pulps have a large fiber length distribution, i.e., the pulp contains long tracheid fibers (2–5 mm) and a relatively high content of fines (short fibers whose length is less than 0.4 mm). Long fibers hinder pulp defibering and fines produce dust [4]. Shorter fibers (e.g., libriforms in hardwood pulps) are easier to defiberize, but these fibers possess a weaker network than long fibers of softwood pulp in air-laid formulations. There is a prominent tendency in some applications to use fluff pulp that is made of hardwood instead of softwood pulp, for example, from *Eucalyptus* kraft pulp [5–7].

The main quality parameters of fluff pulps are related to their absorption capacity, absorption rate, and the air-laid network strength [7–9]. These quality parameters are negatively affected by undefiberized agglomerates (knots) in the fluff pulp. Among the factors that influence the absorption capacity of fluff pulps, the chemical composition of the fibers, the morphology, and their arrangement in air-laid network stand out [5–10]. The intrinsic absorbance of the fibers is related to their accessible surface, which, in turn, depends on the chemical composition and physical structure of the fibers, but also on their length, diameter and stiffness (fiber morphology). An increase in the length and mechanical deformation of the fibers positively contributes to the porosity and burst resistance of the fiber network. However, the importance of changes in the affinity of the fiber surface with water for the absorption capacity in relation to structural changes in the fiber network is not entirely clear. The penetration rate of water into porous fiber network via such important absorption mechanism as capillary suction can be described by the modified Washburn equation [11]:

$$\frac{dl}{dt} = \frac{\gamma_{lv}\, r\, cos\theta}{4\eta l} \tag{1}$$

where l is the distance penetrated into capillary of radius r in time t by a liquid of surface tension γ_{lv} and viscosity η. The contact angle θ between the drop of liquid and the fiber surface reflects the affinity of this liquid to the capillary surface formed by fiber's mesh.

According to Equation (1), an increase in wettability at the fiber-water interface (low θ) causes faster water penetration in the inner layers of the web. At the same time, the larger the average pore size in a given pulp network, the greater is the fluid flux inside the web. The maximum absorption capacity (C_{am}) of a sample with porosity ε and density ρ, for liquid with density ρ_l, per unit mass of dry solid medium, and assuming that there is no change in dimension under wetting and the entire pore space is filled up, can be expressed as follows [12]:

$$C_{am} = \frac{\rho_l}{\rho}\,\frac{\varepsilon}{1-\varepsilon} \tag{2}$$

Because the conditions for the manufacture of kraft pulp (wood pulping and pulp bleaching) affect the chemical composition of the pulp and the morphology of the fibers, these conditions can cause changes in the absorption capacity of the air-laid fiber network. The present work focuses on the characterization of the absorption capacity and affinity of the surface towards water of a set of bleached *Eucalyptus* kraft fluff pulps in order to determine the relationship between the former parameters and the chemical composition and the fiber morphology. Accordingly, fluff pulps were analyzed by capillarity absorption and thermodynamic methods, such as sorption isotherms, sorption enthalpies, and contact angle measurements.

2. Materials and Methods

Six industrially produced eucalypt kraft pulps, cooked, and elementary chlorine free (ECF)/totally chlorine free (TCF) bleached, under conditions that cover all the range of typically applied technological

parameters at the CELBI kraft pulp mill (Leirosa, Portugal), were used in this study. The chemical analysis of kraft pulps (carboxylic group content (CG) and monosaccharide composition) and their fiber morphology were determined, as described previously [7]. Thus, CG was determined by conductometric titration according to the SCAN-CM 65:02 standard method. The sugar analysis was carried out as alditol acetates by GC after two-step Saeman hydrolysis. The morphology of the fibers after defiberization was analyzed using a Kajaani FS300 fiber analyzer (Espoo, Finland). Pulps were dry-defiberized by two-step passage in a pilot-scale Hammermill (Schuttle Buffalo, Model W6H, Buffalo, NY, USA) operated at 3500 rpm. Knot percentage was determined using a RETSCH® sieve shaker adapting to the norm SCAN-CM 37:85. The results of chemical composition and fiber morphology of pulps are presented in Tables 1 and 2, respectively.

Table 1. Carboxylic groups content (CG) and monosaccharide composition of pulps.

Pulp	[CG] (μmol/g)	Monosaccharide Composition (%) *					
		Glu	Xil	Man	Gal	Ara	Ram
1	92.0 ± 1.2	74.4	24.6	0.2	0.2	0.1	0.5
2	128.0 ± 1.9	72.6	26.4	0.3	0.2	0.1	0.4
3	84.0 ± 0.9	76.3	22.9	0.2	0.2	0.1	0.3
4	98.0 ± 0.9	72.2	26.8	0.2	0.2	0.1	0.5
5	116.0 ± 1.5	71.4	27.5	0.2	0.2	0.1	0.6
6	120.0 ± 1.9	72.4	26.3	0.4	0.2	0.4	0.3

* Sugars designations are as follows: glucose (Glu), xylose (Xil), mannose (Man), galactose (Gal), arabinose (Ara) and ramnose (Ram). The relative error in sugars analysis not exceeded of 3–5%.

Table 2. Fiber morphology parameters of defiberized eucalypt kraft fluff pulps.

Pulp	Fiber Length (mm)	Fiber Width (μm)	Fines (%)	Curl (%)	Kink (%)	Coarseness (mg/m)
1	0.781 ± 0.003	18.2 ± 0.01	30.7 ± 0.2	9.9 ± 0.1	45.3 ± 0.1	0.0703 ± 0.001
2	0.771 ± 0.002	17.7 ± 0.01	29.6 ± 0.4	11.0 ± 0.1	49.5 ± 0.2	0.0714 ± 0.003
3	0.775 ± 0.002	18.0 ± 0.01	30.8 ± 0.3	11.5 ± 0.1	50.2 ± 0.1	0.0710 ± 0.003
4	0.773 ± 0.003	17.9 ± 0.01	30.5 ± 0.4	12.0 ± 0.1	52.1 ± 0.3	0.0734 ± 0.004
5	0.776 ± 0.002	17.9 ± 0.01	29.9 ± 0.2	11.6 ± 0.1	50.0 ± 0.2	0.0710 ± 0.006
6	0.758 ± 0.004	17.8 ± 0.01	30.5 ± 0.3	12.8 ± 0.1	53.3 ± 0.2	0.0720 ± 0.005

Water sorption isotherms of defiberized kraft pulps without knots (**1**–**6** pulps) and of **2** pulp with knots (**2K** pulp) were obtained at 25, 30, and 35 °C and at relative pressure in the range between 0.05 and 0.95, while using the Dynamic Vapor Sorption Analyzer (DVS Adventure, Surface Measurement Systems Ltd., Wembley, UK). The experimental sorption data, i.e., equilibrium moisture content, X_{eq} and water activity (or relative pressure), a_w were fitted into the Guggenheim-Anderson-de Boer (GAB) model, since it is valid for high relative pressures ($P/P_0 \leq 0.90$, where P_0 represents the saturation pressure) and proves adequate for surface affinity studies of cellulosic pulps [13,14]. Equation (3) represents this model:

$$X_{eq} = \frac{X_m\, C\, K\, a_w}{((1 - K\, a_w)(1 + (C - 1)K\, a_w))}, \quad (3)$$

where C and K are the GAB model parameters that are related to the heat of sorption in monolayer and in multilayer, respectively, and X_m is the monolayer capacity [13–19]. C, K, and X_m were estimated from the experimental results by non-linear regression analysis:

$$\frac{a_w}{X_{eq}} = \frac{(1 - C)K}{X_m\, C} a_w{}^2 + \frac{C - 2}{X_m\, C} a_w + \left(\frac{1}{X_m\, C\, K}\right) \quad (4)$$

Sorption enthalpies, ΔH_C and ΔH_K, and entropic accommodation factors between mono and multilayer, C_0, and between bulk liquid and multilayer of water molecules, K_0, as determined from Equations (5) and (6) [14,15,20]:

$$\ln\ C = \ln\ C_0\ + \frac{\Delta H_K}{R\,T} \tag{5}$$

$$\ln\ K = \ln\ K_0\ + \frac{\Delta H_K}{R\,T} \tag{6}$$

The net isosteric heat of sorption, ${Q_{st}}^{net}$, was obtained employing the Clausius–Clapeyron equation [14,15,21–25]:

$$\ln\ a_w = \left[\frac{-{Q_{st}}^{net}}{R}\frac{1}{T} + constant\right]_{X_{eq}} \tag{7}$$

However, because the sorption data were not determined at constant moisture content, a_w was calculated from Equation (8) for each X_{eq} value, at different temperatures, while using the GAB parameters that were obtained from experimental data [15,25].

$$a_w = \frac{2 + \left(\frac{X_m}{X_{eq}} - 1\right)C - \left(\left(2 + \left(\frac{X_m}{X_{eq}} - 1\right)C\right)^2 - 4(1 - C)\right)^{\frac{1}{2}}}{2\,K\,(1 - C)} \tag{8}$$

The fraction of occupied sites in the monolayer, ξ^{l_1} was calculated according to Equation (9) [8,16]:

$$\xi^{l_1} = \frac{C\,K\,a_w}{1 + (C - 1)\,K\,a_w} \tag{9}$$

Contact angles were measured on laboratory handsheets (65 g/m^2 ± 2 g/m^2) prepared from **1–6** pulps**,** using a semi-automatic Rapid–Köthen sheet former, according to ISO 5269-1 standard procedure. The measurements were carried out in a Contact Angle System OCA20 goniometer (Data Physics, Filderstadt, Germany) that was equipped with a CCD camera and SCA20 software, while using the sessile drop method applying 3µL micro-drops of distilled water. At least 20 determinations were done per each sample and the obtained results were averaged.

The absorption tests were performed according to the Scandinavian procedure SCAN-C33:80 while using air-laid pads produced from pulps without knots (**1–6** pads) and with knots (**1K–6K** pads). Simultaneously, the specific volume, v, absorption capacity,C_{abs}, and the absorption time, t, have been determined. This testing procedure allows for calculating the total volume (V_t) of each formed pulp pad and, therefore, determine its porosity, ε, according to Equation (10):

$$\varepsilon = \frac{V_t - \frac{m}{\rho}}{V_t}, \tag{10}$$

where m is the dry mass of the pulp pad and ρ is its intrinsic density, calculated as a weighted average of cellulose and xylose densities. The Xylan density was assumed to be equal to 1.20 g/cm^3 and the density of crystalline and amorphous cellulose of 1.59 and 1.40 g/cm^3, respectively [14]. It was assumed that the average degree of crystallinity of cellulose in *Eucalyptus* kraft pulp is 71% [14]. The proportions of xylan and cellulose (glucan) were inferred from the sugar composition of pulp that is presented in Table 1.

Multivariate analysis between surface and capillarity absorption properties of the studied pulps and their chemical composition and fiber morphology were obtained by principal component analysis, while using JMP14 software [26].

3. Results and Discussion

3.1. Sorption Isotherms and Sorption Enthalpies

Sorption isotherms for **1**–**6** pulps and the **2K** pulp, at 25 °C, 30 °C, and 35 °C are presented in Figures 1 and 2, respectively. The obtained isotherms are consistent with type II isotherms, typical of hydrophilic polymers, such as cellulose, possessing free hydroxyl groups, which are largely responsible for water sorption [14,27]. An increase in temperature induces a reduction in the equilibrium moisture content at a specific water activity, being more significant at higher a_w values, as should be expected for fibrous cellulosic materials [15,28]. The increase in the temperature increases the state of excitation of the water molecules and, consequently, decreases the attractive forces between them, due to an increase between their mutual distances. This decrease in binding energy between water molecules and the surface of the absorbent material results in the breakdown of these bonds, and, therefore, in a decrease of the equilibrium moisture content for a given water activity value. Figure 2 also shows that knots content did not significantly affect the equilibrium moisture content. This means that fibers in bundles maintained the accessibility comparable with that of well-separated fibers. In practice, inaccessible surfaces of aggregated fibers in cellulosic materials become accessible via the cleavage of intermolecular hydrogen bonds by water, thus promoting fiber swelling and increasing the effective surface area [14,19]. Hence, the agglomeration of fibers is not a problem for their accessibility inside the knots.

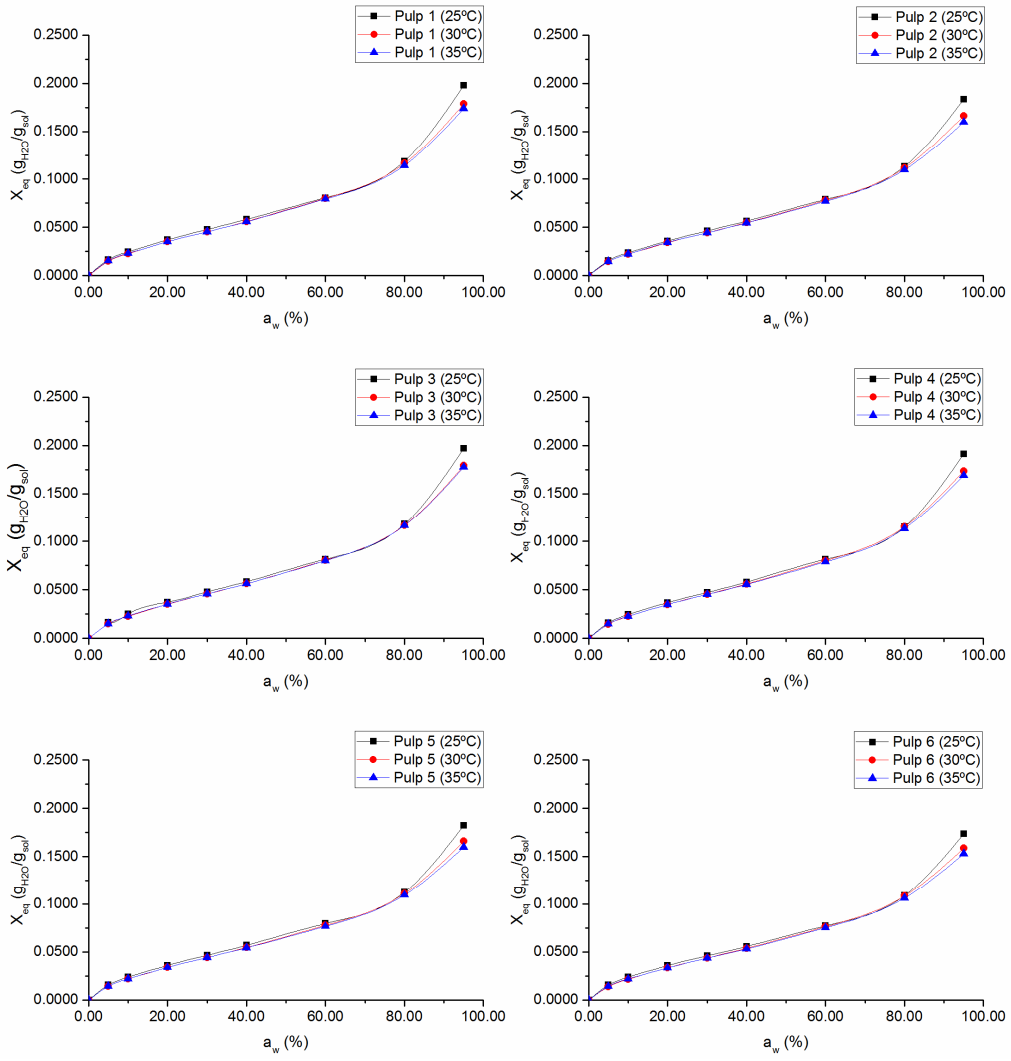

Figure 1. Sorption isotherms of pulps **1**–**6** without knots at 25, 30, and 35 °C.

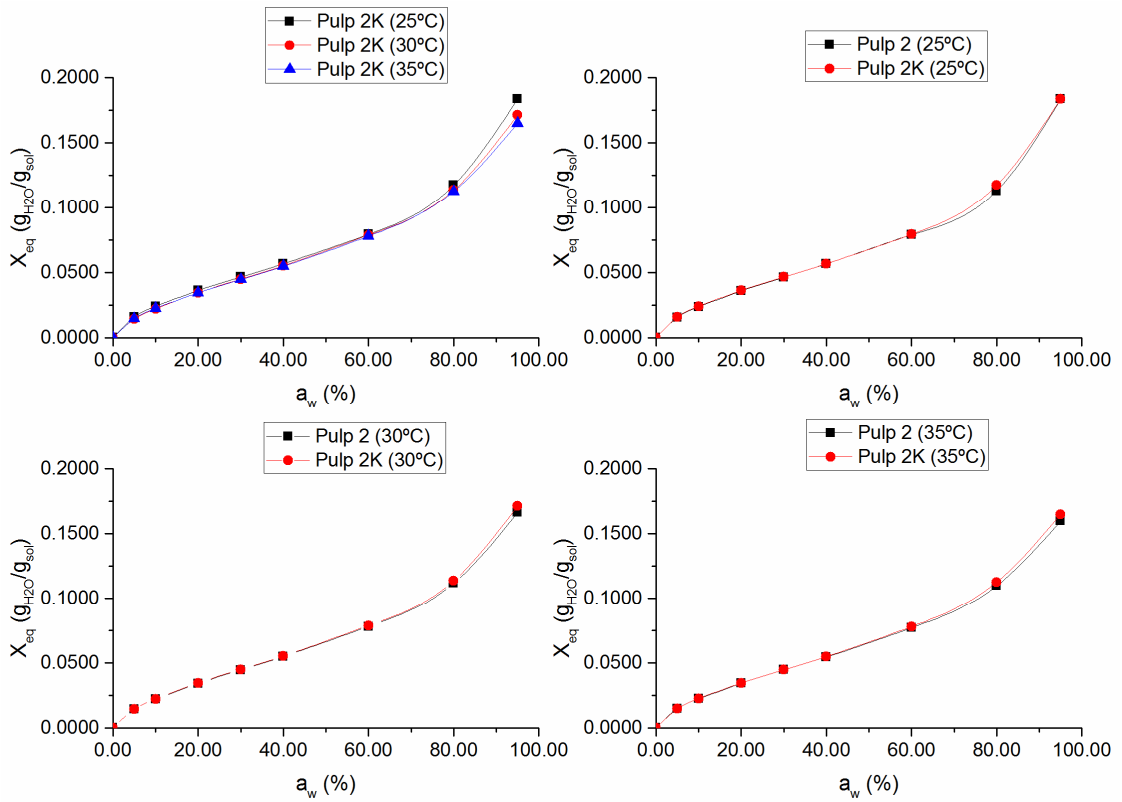

Figure 2. Sorption isotherms of fluff pulps with knots (**2K** pulp) and without knots (**2** pulp) at 25, 30, and 35 °C.

The sorption isotherms allow for evaluating the capacity of the monolayer (X_m) in the fluff pulp, while adjusting the GAB model to the experimental data and infer the effective parameters (Equations (3) and (4)). Only "free" hydroxyl groups not involved in strong intramolecular and intermolecular hydrogen bonding bind water molecules, thus forming a monolayer at low water activities ($a_w \leq 0.40$) [27,28]. This monolayer is discontinuous, because of randomly distributed free hydroxyl groups and their differences in accessibility. Bleached *Eucalyptus* kraft pulps contain notable amounts of glucuronoxylan, which is located essentially in the outer layers of the fibers [29]. Accordingly, the content of xylan and its chemical structure (mainly the quantity of uronic moieties) contribute to the absorption of water by the fluff pulps and must be considered in the interpretation of the results of the isothermal sorption.

Table 3 presents the obtained monolayer capacity values. This parameter measures the availability of active sites on the material for water sorption to occur [14–16] and it was used to estimate the specific surface area of the absorbent material, S as Equation (11):

$$S = \frac{X_m \, N_A \, A_m}{M} \tag{11}$$

where M is the water molecular weight, N_A the Avogadro number, and A_m the effective cross-sectional area of the water molecule (0.125 nm^2 for water at 298 K) [21]. X_m values and, consequently, S values decrease with temperature (Table 4). This result is in accordance with considerations of other studies that attributed this issue to a reduction in the total number of active sites for water binding as a result of physical or chemical changes on the fiber surface that is induced by temperature [14–21,28].

Table 3. Monolayer capacity values at 25, 30, and 35 °C.

	$X_m \pm dX_m$ $(\frac{g_{H_2O}}{g_{sol}})$		
Pulp	**T = 25 °C**	**T = 30 °C**	**T = 35 °C**
1	0.048 ± 0.002	0.046 ± 0.003	0.046 ± 0.003
2	0.047 ± 0.003	0.046 ± 0.003	0.046 ± 0.003
3	0.047 ± 0.003	0.047 ± 0.003	0.047 ± 0.003
4	0.048 ± 0.004	0.047 ± 0.003	0.046 ± 0.003
5	0.048 ± 0.003	0.046 ± 0.003	0.046 ± 0.003
6	0.047 ± 0.003	0.046 ± 0.003	0.045 ± 0.003
2K	0.047 ± 0.002	0.046 ± 0.002	0.045 ± 0.003

Table 4. Specific surface area of pulps at 25, 30 and 35 °C.

	$S \pm dS$ $(\frac{m^2}{g_{sol}})$		
Pulp	**T = 25 °C**	**T = 30 °C**	**T = 35 °C**
1	201 ± 8	194 ± 15	191 ± 12
2	196 ± 12	193 ± 15	191 ± 12
3	198 ± 12	195 ± 15	195 ± 12
4	200 ± 16	196 ± 15	193 ± 13
5	199+ ± 14	194 ± 15	191 ± 13
6	195 ± 11	192 ± 15	189 ± 11
2K	197 ± 7	194 ± 14	190 ± 12

Energy parameters *C* and *K* of the GAB sorption model are shown in Tables 5 and 6, respectively. Parameter *C* is essentially related to differences in enthalpy between monolayer (H_1) and multilayer (H_n), and it measures the binding energy of the forces between water molecules and the fiber surface [14–19]. The *C* values presented in Table 5 suggest that the effective binding force between water molecules and the surface of agglomerated and compact fibers (knots) is weaker than between water molecules and non-agglomerated fibers, since the *C* value for **2K** pulp is lower in comparison to *C* value for **2** pulp. Parameter *K* is related to differences between enthalpy in the bulk liquid (H_L) and multilayer [14,15]. *K* varies between 0 and 1; when it approaches one, water molecules that are beyond the monolayer are not structured in a multilayer and there is almost no distinction between multilayer molecules and bulk liquid. The lower the *K* value, the more sorbed molecules are structured in a multilayer [14,15]. The *K* values are very similar for all samples, varying in the range between 0.7 and 0.8 (Table 6), which indicate that the multilayer is structured and its properties are distinct from the bulk liquid [14]. The temperature has negative effect on *C* and positive effect on *K*, as it has already been reported for other cellulosic materials [14,15,28]. These results are consistent with the definition of these parameters, i.e., C decreases with increasing temperature due to the decreasing of monolayer binding energy and K increases with increasing temperature, which indicates that multilayer water molecules become more similar to those in bulk liquid, due to the increase of their excitation state.

Table 5. Energy parameter *C* at 25, 30, and 35 °C.

	$C \pm dC$ **(adm)**		
Pulp	**T = 25 °C**	**T = 30 °C**	**T = 35 °C**
1	10.7 ± 0.6	10.0 ± 0.9	9.8 ± 0.7
2	11.0 ± 0.5	9.9 ± 0.9	9.5 ± 0.7
3	12.0 ± 0.5	10.0 ± 0.9	9.5 ± 0.7
4	11.0 ± 0.5	9.9 ± 0.9	9.4 ± 0.7
5	11.0 ± 0.5	9.6 ± 0.9	9.4 ± 0.7
6	11.5 ± 0.5	9.8 ± 0.9	9.4 ± 0.6
2K	10.4 ± 0.4	9.8 ± 0.8	9.5 ± 0.7

Table 6. Energy parameter *K*. at 25, 30, and 35 °C.

	$K \pm dK$ (adm)		
Pulp	**T = 25 °C**	**T = 30 °C**	**T = 35 °C**
1	0.77 ± 0.05	0.78 ± 0.09	0.80 ± 0.08
2	0.76 ± 0.07	0.77 ± 0.09	0.78 ± 0.08
3	0.78 ± 0.07	0.78 ± 0.09	0.80 ± 0.07
4	0.76 ± 0.09	0.77 ± 0.09	0.79 ± 0.08
5	0.75 ± 0.08	0.77 ± 0.09	0.78 ± 0.08
6	0.75 ± 0.07	0.76 ± 0.09	0.78 ± 0.07
2K	0.78 ± 0.04	0.77 ± 0.08	0.80 ± 0.07

Enthalpy differences and entropy accommodation factors between monolayer and multilayer ($\Delta H_C = H_1 - H_n$ and C_0, respectively), and between bulk liquid and the multilayer ($\Delta H_K = H_L - H_n$ and K_0, respectively) revealed that ΔH_C are positive (Table 7), because the interaction of water with primary sorption sites is exothermic [15]. ΔH_K. values are smaller, because multilayer molecules interact less than monolayer molecules with the surface of the absorbent material and, consequently, multilayer molecules are less firmly bounded in comparison to the monolayer molecules [14–16]. These results show that the enthalpy that is associated with adsorbed water molecules follows the order: $H_1 > H_n > H_L$, i.e., the interactions of water molecules in the monolayer are stronger in comparison with the multilayer. The C_0 values are smaller than 1, because, from an entropic point of view, the water molecules have a larger degree of freedom in the multilayer. Similarly, the K_0 values are greater than 1 due to higher molecule's entropy of the molecules in the bulk liquid. K_0. values are larger than C_0 values because of a more significant entropic contribution due to the strongly increased number of configurations and mobility of molecules in the bulk liquid compared to molecules in the multilayer.

Table 7. Enthalpy differences and entropic accommodation factors between the monolayer and multilayer (ΔH_C, C_0) and between the bulk liquid and the multilayer (ΔH_K, K_0).

Pulp	$\Delta H_C \pm d\Delta H_C$ **(kJ/mol)**	$C_0 \pm dC_0$ **(adm)**	$\Delta H_K \pm d\Delta H_K$ **(kJ/mol)**	$K_0 \pm dK_0$ **(adm)**
1	7 ± 1	0.5 ± 0.2	−3.3 ± 0.2	2.9 ± 0.2
2	12 ± 3	0.2 ± 0.01	−2.1 ± 0.6	1.7 ± 0.4
3	16 ± 4	0.02 ± 0.01	−2.4 ± 0.6	2.0 ± 0.5
4	13 ± 3	0.2 ± 0.01	−3.0 ± 0.4	2.6 ± 0.4
5	13 ± 5	0.2 ± 0.01	−2.7 ± 0.2	2.3 ± 0.2
6	16 ± 5	0.02 ± 0.01	−2.9 ± 0.4	2.4 ± 0.4
2K	7 ± 1	0.7 ± 0.03	−2.0 ± 0.9	2.0 ± 1.0

The net isosteric heat of sorption is an important thermodynamic parameter, which measures the binding energy of the forces between the water vapor molecules and the absorbent material. It gives useful information regarding the sorption mechanism, since it can help to interpret the type of water binding that is occurring at a given moisture content [15,16,30–33]. The results presented in Figure 3 show the existence of three classes of water with a continuous transition from tightly bound water to free water molecules. In the monolayer region, water molecules are tightly bound to the material, corresponding to high interaction energy (high Q_{st}^{net} values). At increasing moisture content, net isosteric heat of sorption decreases, since most active sites become occupied and sorption occurs on the less active sites, which results in lower heats of sorption. Ultimately, Q_{st}^{net} approaches zero, which indicates that the total heat of sorption is equal to the heat of vaporization of pure water, i.e., the region where adsorbed water molecules behave as molecules in the liquid state with properties like those of the bulk liquid. The knots effect is well evidenced in Figure 3 for **2K** pulp, as there is a noticeable decrease in isosteric heat of adsorption in the monolayer region. This result is in accordance with the previous conclusion, i.e., the binding energy between aggregated fibers in knots and water molecules is weaker when compared to well-separated fiber-water binding forces. The maximum net isosteric

heat of sorption, which can be theoretically defined as $Q_{st,max}^{net} = \Delta H_C + |\Delta H_k|$ [14], can be associated to physical interpretation of GAB parameters: Q_{st}^{net} and ΔH_C are related to sorption energy in monolayer and ΔK is related to multilayer interactions. In fact, a higher monolayer sorption enthalpy (ΔH_C) corresponds to a higher value of $Q_{st,max}^{net}$ (e.g., in the case of **3** and **6** pulps, Figure 3). It was also found a clear relation between Q_{st}^{net} and $|\Delta H_K|$: **3** and **6** pulps have the lowest multilayer sorption enthalpy, i.e., lower $|\Delta H_K|$ and, consequently, Q_{st}^{net} reaches zero at lower moisture content, demonstrating that these have a less structured multilayer and their water molecules have properties that are similar to bulk liquid.

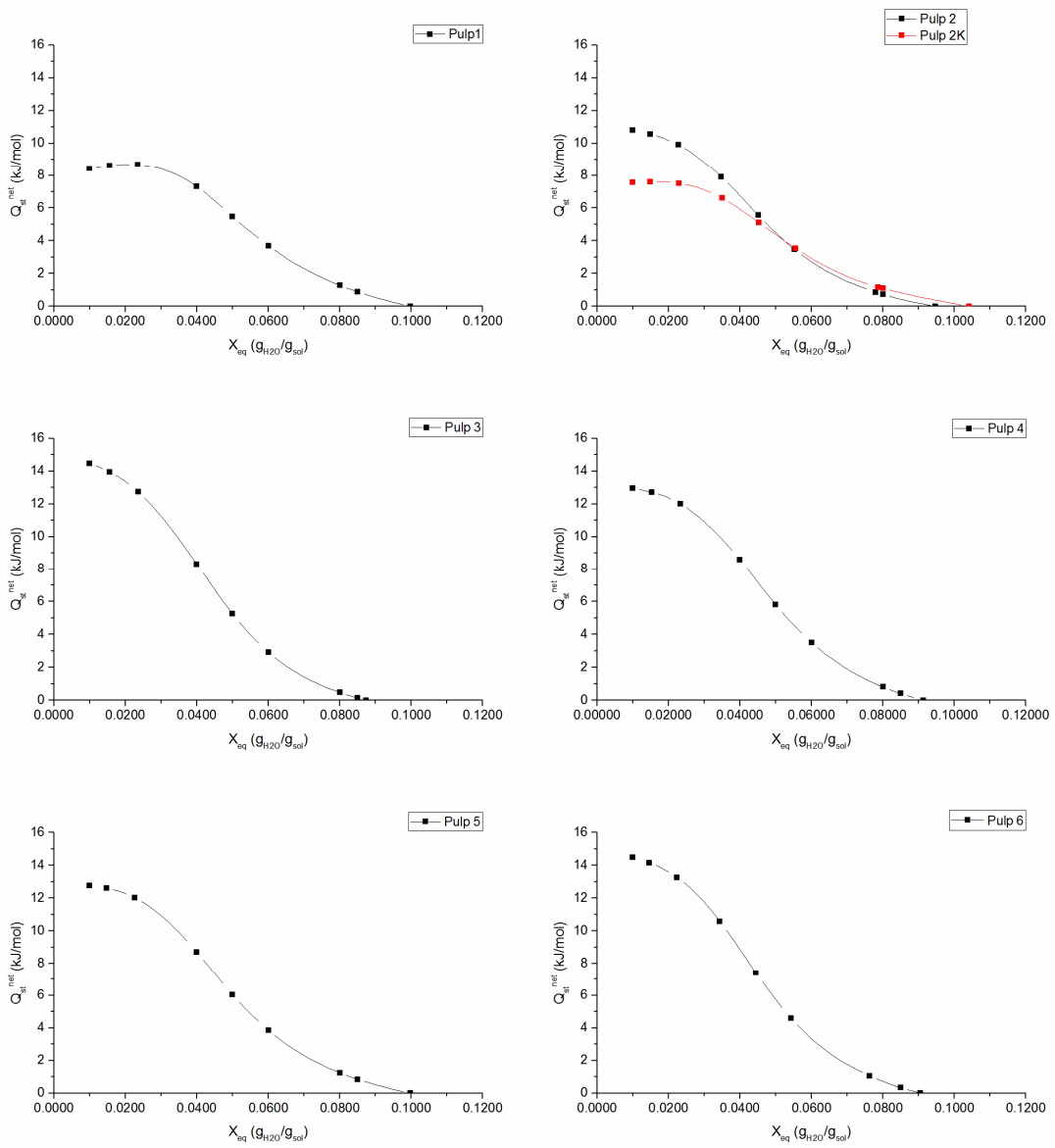

Figure 3. Net isosteric heat of sorption as function of moisture content derived from experimental sorption data for each pulp.

The fraction of occupied sites in the monolayer, ξ^{l_1}, plotted as a function of water activity, evidences the assumption of incomplete surface coverage of the adsorbent material and the formation of the multilayer (Figure 4). At low water activity values, the surface has more available sites for the water molecules to form hydrogen bonds with the surface and, therefore, there is a more pronounced growth in ξ^{l_1} at low relative pressure (up to a_w = 40%). As the monolayer of water molecules forms, the surface becomes less accessible due to the "jamming" of the adsorbate water molecules, favoring bonds

between water molecules instead of bonds between water molecules and the surface [21]. For each pulp, the maximum fraction of occupied sites in the monolayer is higher than 96%, which indicates good surface affinity of the absorbent material for water molecules. As could be expected, by analogy with X_m, ξ^{l_1} values were negatively affected by temperature, especially at relatively low a_w ($\leq$ 40%) (Figure 4).

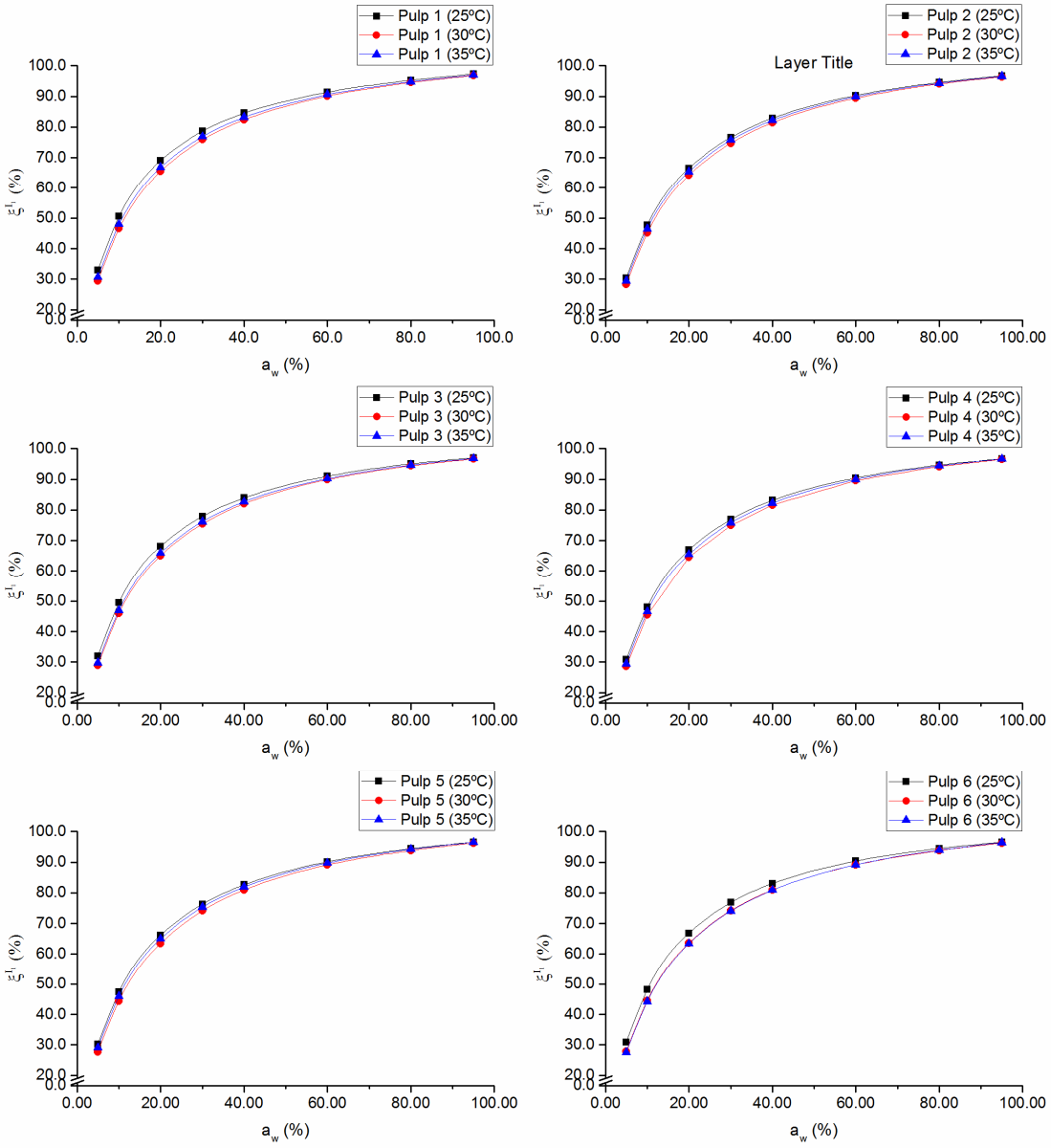

Figure 4. Fraction of occupied sites in the monolayer (ξ^{l_1}) for **1–6** pulps as a function of water activity at 25, 30, and 35 °C.

3.2. *Contact Angles of Pulps*

Contact angles, θ, were measured on laboratory pulp handsheets with smooth surface in order to minimize the effect of surface roughness. At least similar roughnesses were detected for all samples when evaluated by known Bendtsen test according to ISO 8791/2:2013, making the results of contact angle tests comparable. Contact angles varied between 17° and 27° (Figure 5), thus demonstrating common strong pulp wettability, as solid-liquid attraction largely prevailed over the liquid-liquid one [34]. The contact angles, that reflect the wettability of the handsheet surface, must relate to the affinity of the pulp fibers for water (i.e., X_m and S). Figure 5 shows that the wettability of the

handsheet's surface is clearly related to fiber's affinity for water: the sheet with lower contact angle has been produced from the pulp that has better ability to retain water molecules on their surface (higher value of X_m). Hence, a surface with fibers that are more accessible to form hydrogen bonds with water provides higher hydrophilicity to the pulp, which, in turn, correspond to lower contact angles measured on handsheets formed from it. The experimental results unambiguously confirm that the wettability of the pulp handsheets and the affinity of the fiber surface with water are inextricably related. Pulps with extreme contact angles (e.g., **1** pulp with Θ= 17° and **6** pulp with Θ= 27°, Figure 5) did not correlate univocally with their chemical composition (amount of hemicelluloses or carboxylic moieties, Table 1), or with their basic fiber morphology (average fiber length/width or coarseness, Table 2). On the other hand, a tendency of pulp´s contact angle to increase with fiber´s deformation (curl and kink, Table 2) was clearly traceable (r^2 = 0.7–0.8, figure not shown).

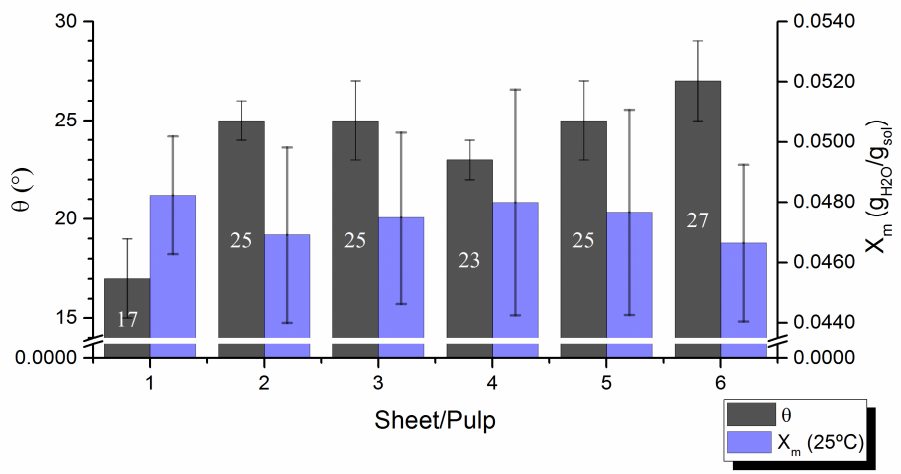

Figure 5. Monolayer capacity (X_m) of **1**–**6** pulps at 25 °C and the average contact angles of corresponding handsheets.

The deformations of the pulp fibers, such as curl and kink, are mostly irreversible being caused by distortion and compression of the fibril layers [35–37]. The misalignment of the fibril lamellas lead to wavy layers (Figure S1, Supplementary Materials), where some adjacent surfaces in the creases approach each other, forming intrafiber cross-links by hydrogen bonding of free hydroxyl groups [37]. As a consequence, the accessible area of the damaged fibers can be slightly reduced, which caused the lower monolayer capacity and the wettability of the fiber mesh, resulting in Θincrease. On the other hand, the surfaces of deformed fibers, which contain partially disordered cellulose fibrils, are more accessible when compared to surfaces of non-deformed fibers [36]. This fact can explain the larger ΔHc (Table 7) and Q_{st}^{net} (Figure 3) of more curled and kinked pulp fibers (Table 2) observed experimentally. These accessible surfaces of deformed fibers can also readily form the intensive hydrogen bonds between the fibers in the handsheets, thus contributing to the reduction in paper surface wettability (increases in Θ). Therefore, the contact angle of the fiber web reflects the apparent wettability of the surface and not necessarily just the intrinsic contribution of the constituent fibers [38]. Nevertheless, the contact angle is one of the most common and reliable analyses for assessing the wettability of cellulosic materials.

3.3. Capillarity Absorption

Porosity (ε), specific volume (v), absorption capacity (C_{abs}), and absorption time (t) of **1**–**6** pads without knots and **1K**–**6K** pads with knots revealed notable differences, depending on the fiber network structure in pads (Table 8). These differences influenced the absorption properties. Thus, the knots turn the fiber network much more compact (less bulky), negatively affecting the porosity of air-laid pads. However, this fact did not lead to the expected drop in C_{abs} of pads formed from knotted pulp

compared to knotless one (Table 8), although within a series of **1–6** or **1K–6K** pads some tendency to decrease of C_{abs} was observed with the decrease in the specific volume of the pad. Furthermore, predicted by Equation (2) the maximal absorption capacity (C_{am}) of pads was more than five times greater than those obtained experimentally. This apparent discrepancy can be explained by the collapse of pad pores upon wetting. The contraction of the volume of the pad occurs essentially under the gravity of the absorbed liquid, due to the low mechanical resistance of the wet mesh [12]. Hence, the C_{abs} depended significantly on the strength of network under wetting. In this context, a certain positive effect of knots on the C_{abs} can be explained by the inclusion of rigid fiber bundles in the network that preserve it from collapse under moistening. As already pointed out, the accessibility of fibers within the knots is not much worse than that of disintegrated fibers (Figure 2). However, the monolayer sorption enthalpy (ΔH_C) and the net isosteric heat of sorption (Q_{st}^{net}) of fibers in knots are lower than those of well-separated fibers (Figure 3 and Table 7), due to the more intense interfiber interactions in the formers. This, together with lower pore size inside than outside of knots, must lead to the lower penetration rate of water into the pad (Equation (1)). Such behavior was experimentally confirmed for most of the evaluated pulps (Table 8).

Table 8. Porosity, specific volume, absorption capacity and absorption time of pads formed from pulps without (**1–6** pads) and with (**1K–6K** pads) knots.

Pad	*Knots (%)*	ε (%)	ν (cm^3/g_{sol})	C_{abs} (g_{H2O}/g_{sol})	t (s/g_{sol})
1	-	98.2 ± 0.1	18.3 ± 0.1	11.0 ± 0.1	0.95 ± 0.01
1K	26.9	97.8 ± 0.1	13.4 ± 0.1	11.2 ± 0.1	0.82 ± 0.01
2	-	98.3 ± 0.1	20.6 ± 0.2	11.3 ± 0.1	0.47 ± 0.01
2K	25.0	98.2 ± 0.1	16.4 ± 0.1	12.2 ± 0.2	0.59 ± 0.01
3	-	98.3 ± 0.1	20.6 ± 0.2	11.1 ± 0.1	0.60 ± 0.01
3K	24.9	98.2 ± 0.1	17.3 ± 0.1	10.8 ± 0.1	0.61 ± 0.01
4	-	98.2 ± 0.1	19.9 ± 0.1	10.9 ± 0.1	0.83 ± 0.01
4K	20.0	98.1 ± 0.1	15.2 ± 0.1	10.7 ± 0.1	0.91 ± 0.01
5	-	98.2 ± 0.1	20.3 ± 0.2	11.1 ± 0.1	0.61 ± 0.01
5K	26.2	98.1 ± 0.1	16.7 ± 0.1	11.4 ± 0.1	0.56 ± 0.01
6	-	98.3 ± 0.1	20.9 ± 0.1	11.6 ± 0.1	0.41 ± 0.01
6K	22.5	98.2 ± 0.1	16.4 ± 0.1	11.7 ± 0.1	0.50 ± 0.01

According to common knowledge, the strength of the network becomes better when using longer, coarser, and curvier fibers [10,12,39]. Among six examined pulps, which were obtained from the same wood specie and by similar processing mode, the fiber length/width and coarseness varied little (Table 2). However, the fiber deformation parameters of pulps (curl and kink) varied quite substantially. The minimal fiber deformations were registered for **1** pulp and the maximal for the **6** pulp. These pulps have the opposite surface affinity for water in terms of X_m, ΔH_C, Q_{st}^{net} and contact angles (Tables 3, 7 and 8 and Figures 3 and 5) and demonstrated the opposite absorption capacity and the absorption rate (Table 8). Contrary to expectations, more hydrophilic **1** pulp showed less absorption capacity and absorption rate than less hydrophilic **6** pulp. The only explanation is the structure of the fiber network of **6** pad, comprised of fibers that are more curled, kinked, and coarser than those of **1** pad, which promoted a more bulky/porous and robust structure than that formed in the **1** pad. Therefore, the structure of the fiber network is a more important factor affecting absorptivity than the intrinsic hydrophilicity of the constituent fibers, at least in the range of contact angles of ca. 15–30°.

On the other hand, the better absorption capacity and the absorption rate of **2** and **6** pulps in relation to **3** and **5** pulps does not match well to the proposition that the structure of the network is a unique dominant factor, because ε, υ, and the main deformation parameters of the fibers in pulps (curl and kink) did not vary significantly as to justify this assumption (Tables 2 and 8). At the same time, **2** and **6** pulps had one of the highest contents of carboxylic groups, which mainly belong to the glucuronoxylan that is present in the pulps (Table 1). The latter suggests that the chemical composition of the fibers also has an important contribution to absorption, because it is known that

hemicelluloses and other components containing carboxylic moieties contribute largely to the swelling of the pulp [10,40]. The swelling of the polymeric network is one of the basic mechanisms in the absorption by porous materials [10,41].

Interestingly, the **4** pulp containing the high amount of the hemicelluloses and carboxyl groups (Table 1) and having the coarsest and most deformed fibers among the examined pulps (Table 2), allowing for porous and bulky pads, showed the worst absorption capacity, and the lowest absorption rate (Table 8). At least partially, these findings can be explained by the smaller number of knots in **4** pulp (Table 8) and one of the shorter lengths of fiber (Table 2).

The relationships between the surface properties of the pulp fibers, their chemical composition, and morphology with respect to the absorption capacity of the resulting air-produced formulations are not straightforward and multi-dependent, as can be seen from the above reasoning. To better trace these relationships, statistical analyzes of the absorption capacity in relation to the pulp properties were performed.

3.4. Multivariate Analysis

Principal component analysis (PCA) was used to monitor the main relationships between the absorption capacity of the studied pulps and their surface properties, chemical composition, and fiber morphology (Figure 6). The PCA reflects the correlation between the variables, expressing their contribution to the two principal components (PC), in terms of relative variation. Thus, two variables that are located at the same quadrant indicate a positive correlation, since them positively or negatively contribute to the two PCs, and this correlation is as stronger as closer they are. When located in opposite quadrants, two variables present have a negative correlation with each other, because they translate into opposite effects for the PCs. When located in parallel quadrants, two variables apparently have the same contribution to one PC and the opposite contribution to the other. However, it is necessary to consider the total variation that is explained by each of the PCs. In this case, component 1 (PC1) explains 69.9%, while the component 2 (PC2) explains only 14.9% of variations (Figure 6). Therefore, the correlations between the different variables will be analyzed, especially in relation to their contribution to PC1 describing mainly the fiber network properties.

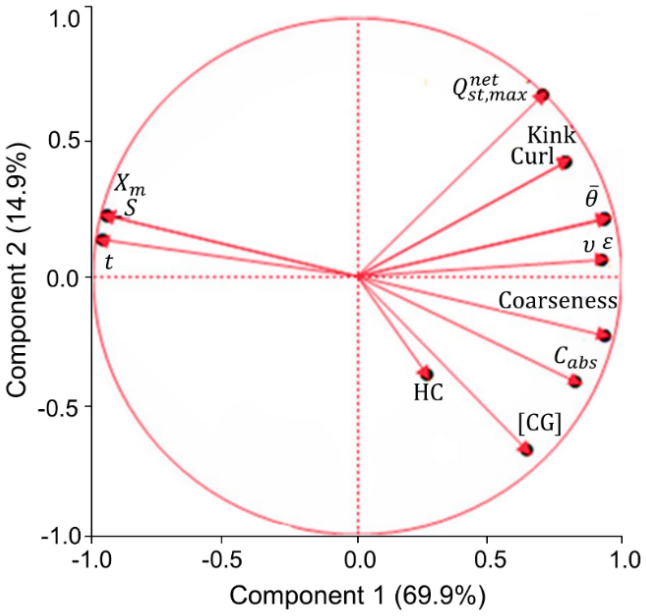

Figure 6. Principal component analysis (PCA) diagram elucidating the structure-property relationships of kraft fluff pulps **1**–**6**.

In general, the PCA supports previous conclusions that the affinity of the fiber surface with water, expressed by X_m and S and the surface wettability (measured by the contact angle, Θ), are not necessarily related to the improved capillarity absorption properties (C_{abs} and t). In fact, statistically, X_m and S have positive correlation with absorption time (t) and negative correlation with absorption capacity (C_{abs}). The opposite effect is verified in relation to the correlations between the average contact angle (θ) and these absorption properties. The PCA also shows that higher coarseness correlated with the lower accessible surface area (S) and the monolayer capacity (X_m) and the increased fiber deformations (kink and curl) to the lesser wettability of handsheet's surface, i.e., larger contact angles (Figure 6). The reasons for such correlations have been previously discussed when analyzing the affinity of the pulp surface with water (Section 3.2) and the relationship between the absorption capacity and the structure of the fiber network in air-laid pads (Section 3.3).

The expectable positive correlation was found regarding the presence of highly hydrophilic components in pulps (hemicelluloses and other polysaccharides containing carboxylic groups) and their absorption capacity (Figure 6). The absorptivity of pulps also positively correlated with fiber coarseness and, to a lesser extent, with curled and kinked fibers. In fact, the network with a higher coarseness of fibers usually exhibits better absorption properties, because these bulky fibers possess less interfiber bonding areas, resulting in a network with high specific volume, high porosity, and, therefore, improved absorbency. The positive contribution of deformed fibers to improve the specific volume (ν) and the porosity (ε) of air-laid pads has also been discussed previously and favored the pulp's absorption capacity. It is worth mentioning that the deformations of the fibers provided the greatest contribution to ν and ε of the pads. These deformations occurred during the production of kraft pulp, due to the variable cooking and bleaching processing conditions. These conditions also affected the chemical composition of pulp due to the variable degradation of hemicelluloses [42]. Dry defibration is another cause of fiber deformation, which depends on the manufacturing history, e.g., pulping and bleaching conditions.

Although the content of hemicelluloses (HC) in pulps is expectedly related to the carboxyl groups content (CG) (Figure 6), a much weaker relationship exists between the HC content and the absorption capacity (C_{abs}). HC usually contributes negatively to the air-laid fiber network strength due to the weakening of wet mesh, thus decreasing the network flexibility and leading to less curled fibers [8]. Consequently, the effect of HC on C_{abs} is not straightforward. On the one hand, HC favors the network swelling and water retention and, on the other hand, HC deteriorate the air-laid fiber network structure and strength.

HC contributed negatively to the wettability of the fibers in pads (negative contribution to PC2), according to the PCA data. Thus, the X_m and HC located, even in the opposite quadrants, indicating a negative correlation with each other (Figure 6). This feature is in line with the known fact that HC can negatively affect the wettability of the fiber web, resulting in an increase in Θ with the extent of HC present in the pulp [38,43,44]. The plausible explanation deals with intensive formation of hydrogen bonds between free hydroxyl groups on the surface of cellulose fibrils and amorphous hemicelluloses. As a result, the amount of free hydroxyl groups in the cellulose fibrils is decreasing and the interfibrillar space is reduced being filled with HC, thus diminishing the monolayer capacity of fibrils. The removal of moderate amounts of hemicelluloses can lead to better wettability of fibers, because the lower the hemicellulose content, the looser the cellulose fibrils network in fiber, and, consequently, fiber mesh will have higher specific volume and higher porosity. However, with a very low HC content, when the fibers are dried intensively, their surface is collapsed due to the intensive aggregation of fibrils within cell wall and the wettability of the fibers decreases [38,40]. Therefore, hemicelluloses can have both positive and negative effects on fiber wettability.

It is noteworthy that, among the studied pulps, the variations in HC content did not exceed 20% and the eventual direct relationship between the decrease in HC content (Table 1) and the increase in Θ of pulp fibers (Table 8) was not clearly detectable. It was recently reported that the capacity of pulp fiber to swell depends not only on the amount of hemicelluloses in eucalypt kraft pulp, but also on

their location within the cell wall [45]. The last feature depended on the pulping severity, mainly the alkali load and the cooking temperature. Hence, it is reasonable to propose that the wettability and absorption capacity of kraft pulps in study also depended not only on the HC content, but also on the HC distribution in the cell wall of fibers.

4. Conclusions

The results of this work showed that the surface properties of industrially produced *Eucalyptus* kraft fluff pulp varied noticeably within the range of process conditions applied to the mill. In addition to wettability, the pulp fibers revealed significant morphological changes, mainly related to their deformations. The processing conditions also induced nearly 20% variability in knots content upon dry-defiberization of kraft pulps.

Despite the similar accessibility of non-agglomerated fibers and fibers agglomerated in knots, the latter have less isosteric heat of adsorption in the monolayer than the former and, therefore, possess less wettability. This, together with relatively low porosity, reduces the absorption capacity and increases the absorption times of air-laid formulations containing knots. At the same time, the better wettability of the fiber surface not necessarily related to the improved capillary absorption. The last largely depended on the fiber network structure, which, in turn, is affected by fiber morphology and the chemical composition of the pulp. The highly porous fiber network possessing high network strength and, less deformable when wetted, meets the best requirements for that purposes. The pulp production conditions favoring more coarse and deformed fibers (curled and kinked) are of great preference to produce a fluff pulp with good absorption capacity. The deformed fibers showed less monolayer capacity and the accessible surface, but higher isosteric heat of adsorption in the monolayer, when compared to non-deformed fibers. The last fact was explained by more disordered cellulose fibrils on the surface of deformed fibers, due to the distortion, compression, or even partial rupture of cellulosic lamellas.

The effect of hemicelluloses on fluff pulp adsorption is quite ambiguous. Despite improved water retention by hemicellulose-rich fibers, hemicelluloses provide less wettable fiber surface and weaken the air-laid fiber network under humidification. According to literature evidences, hemicelluloses decrease the deformability of fibers, thus resulting in less porous and less strong fiber network in air-laid formulations. Accordingly, the industrial conditions leading to pulps with diminished hemicelluloses content can be advantageous for the absorption properties of fluff pulps.

However, additional work is needed to more clearly trace the relationships between the fiber surface properties and their network parameters and absorptivity, using pulps from different production histories with a wider range of variation in the chemical composition and morphology of the fiber.

Supplementary Materials: The following supplementary data are available online at http://www.mdpi.com/2571-9637/3/3/20/s1, Figure S1: Schematic representation of a cellulosic fiber possessing curl (A) and kink (B) deformations.

Author Contributions: Conceptualization, D.V.E. and F.M.L.F.; Methodology, D.V.E., S.M.C.R., E.M.D. and F.M.L.F.; Investigation, C.A.A., E.M.D. and S.M.C.R.; Writing—original draft preparation, C.A.A. and S.M.C.R.; Writing—review and editing, D.V.E., E.M.D. and F.M.L.F.; Supervision, D.V.E. and F.M.L.F.; Funding acquisition, D.V.E. and S.M.C.R. All authors have read and agreed to the published version of the manuscript.

Funding: This work was developed within the scope of the project CICECO-Aveiro Institute of Materials, UIDB/50011/2020 & UIDP/50011/2020, financed by national funds through the Portuguese Foundation for Science and Technology/MCTES. The financial and technical support by CELBI S.A. is greatly acknowledged.

Conflicts of Interest: The authors declare no conflict of interest.

References

1. Young, D.; Barlow, F. Past, Present and Future of the Global Fluff Pulp Market. *Nonwovens World* **2007**, *16*, 51–56.
2. Fluff Pulp Market Description. Available online: https://www.beroeinc.com/category-intelligence/fluff-pulp-market/ (accessed on 26 February 2019).
3. van Doremalen, N.; Bushmaker, T.; Morris, D.H.; Holbrook, M.G.; Gamble, A.; Williamson, B.N.; Tamin, A.; Harcourt, J.L.; Thornburg, N.J.; Gerber, S.I.; et al. Aerosol and Surface Stability of SARS-CoV-2 as Compared with SARS-CoV-1. *N. Engl. J. Med.* **2020**. [CrossRef]
4. Parham, R.A.; Hergert, H.L. Fluff pulp—A review of its development and current technology. *Pulp Pap.* **1980**, *54*, 110–115.
5. Jordao, M.; Neves, J. Avaliação de pastas lignocelulósicas para fins absorventes com ênfase em pasta fofa (fluff pulp). *O Pap.* **1989**, *2*, 53–62.
6. Eucafluff. Available online: https://www.celuloseonline.com.br/suzano-anuncia-entrada-no-segmento-de-celulose-fluff-de-fibra-curta/ (accessed on 27 September 2019).
7. Rebola, S.M.; Ferreira, J.; Margalho, L.; Jorge, S.R.; Evtuguin, D.V. Potential of bleached eucalypt kraft pulp for new non-papermaking applications. In Proceedings of the XXIV TECNICELPA—Conferência Internacional da Floresta, Pasta e Papel, Aveiro, Portugal, 11–12 October 2018.
8. Lund, K.; Sjoström, K.; Brelid, H. Alkali extraction of kraft pulp fibers: Influence on fiber and fluff pulp properties. *J. Eng. Fiber Fabrics.* **2012**, *7*, 30–39. [CrossRef]
9. Brill, J.W. New Scandinavian fluff test methods. *Tappi J.* **1983**, *66*, 45–48.
10. Hubbe, M.A.; Ayoub, A.; Daystar, J.S.; Venditti, R.A.; Pawlak, J.J. Enhanced absorbent products incorporating cellulose and its derivatives: A review. *BioResources* **2013**, *8*, 6556–6629. [CrossRef]
11. Roberts, J.C. *The Chemistry of Paper*; RSC: Cambridge, UK, 1996; pp. 52–68. ISBN 0-85404-518-X.
12. Chatterjee, P.K.; Gupta, B.S. Porous structure and liquid flow models. In *Absorbent Technology*, 1st ed.; Chatterjee, P.K., Gupta, B.S., Eds.; Elsevier: Amsterdam, The Netherlands, 2002; pp. 1–55, ISBN 0-444-50000-6.
13. Timmermann, E.O. Multilayer sorption parameters: BET or GAB values? *Colloids Surf. A* **2003**, *220*, 235–260. [CrossRef]
14. Portugal, I.; Dias, V.M.; Duarte, R.F.; Evtuguin, D.V. Hydration of Cellulose/Silica Hybrids Assessed by Sorption Isotherms. *J. Phys. Chem. B* **2010**, *114*, 4047–4055. [CrossRef]
15. Quirijns, E.J.; van Boxtel, A.J.; van Loon, W.K.; van Straten, G. Sorption isotherms, GAB parameters and isosteric heat of sorption. *J. Sci. Food Agric.* **2005**, *85*, 1805–1814. [CrossRef]
16. Saadi, R.; Saadi, Z.; Fazaeli, R.; Fard, N.E. Monolayer and multilayer adsorption isotherm models for sorption from aqueous media. *Korean J. Chem. Eng.* **2015**, *32*, 787–799. [CrossRef]
17. Al-Muhtaseb, A.H.; McMinn, W.A.M.; Magee, T.R.A. Moisture Sorption Isotherm Characteristics of Food Products: A Review. *Food Bioprod. Process.* **2002**, *80*, 118–128. [CrossRef]
18. Brunauer, S.; Deming, L.S.; Deming, W.E.; Teller, E. On a Theory of the van der Waals Adsorption of Gases. *J. Am. Chem. Soc.* **1940**, *62*, 1723–1732. [CrossRef]
19. Robens, E.; Dąbrowski, A.; Kutarov, V.V. Comments on surface structure analysis by water and nitrogen adsorption. *J. Therm. Anal. Calorim.* **2004**, *76*, 647–657. [CrossRef]
20. Hossain, M.D.; Bala, B.K.; Hossain, M.A.; Mondol, M.R.A. Sorption isotherms and heat of sorption of pineapple. *J. Food Eng.* **2001**, *48*, 103–107. [CrossRef]
21. Monleón Pradas, M.; Salmerón Sánchez, M.; Gallego Ferrer, G.; Gómez Ribelles, J.L. Thermodynamics and statistical mechanics of multilayer adsorption. *J. Chem. Phys.* **2004**. [CrossRef] [PubMed]
22. Van den Berg, C. Vapour Sorption Equilibria and Other Water-Starch Interactions: A Physico-Chemical Approach. Ph.D. Thesis, Wageningen University & Research, Wageningen, The Netherlands, 1981.
23. Maskan, M.; Karatag, S. Sorption Characteristics of Whole Pistachio Nuts (Pistacia Vera L.). *Dry. Technol.* **1997**, *15*, 1119–1139. [CrossRef]
24. Cadden, A.-M. Moisture Sorption Characteristics of Several Food Fibers. *J. Food Sci.* **1988**, *53*, 1150–1155. [CrossRef]
25. Tsami, E.; Maroulis, Z.B.; Marinos-kouris, D.; Saravacos, G.D. Heat of sorption of water in dried fruits. *Int. J. Food Sci. Technol.* **1990**, *25*, 350–359. [CrossRef]

26. SAS Institute Inc JMP Statistical Software—Free Trial Download. Available online: https://www.jmp.com/en_gb/offers/free-trial.html (accessed on 26 June 2019).
27. Fengel, D.; Wegener, G. Cellulose. In *Wood: Chemistry, Ultrastructure, Reactions*; Walter de Gruyter: Berlin, Germany, 1984; pp. 66–105, ISBN 9780899255934.
28. Parker, M.E.; Bronlund, J.E.; Mawson, A.J. Moisture sorption isotherms for paper and paperboard in food chain conditions. *Packag. Technol. Sci.* **2006**, *19*, 193–209. [CrossRef]
29. Gomes, T.M.P.; Mendes de Sousa, A.P.; Belenkiy, Y.I.; Evtuguin, D.V. Xylan accessibility of bleached eucalypt pulp in alkaline solutions. *Holzforschung* **2020**, *74*, 141–148. [CrossRef]
30. McLaughlin, C.P.; Magee, T.R.A. The determination of sorption isotherm and the isosteric heats of sorption for potatoes. *J. Food Eng.* **1998**, *35*, 267–280. [CrossRef]
31. Palou, E.; López-Malo, A.; Argaiz, A. Effect of temperature on the moisture sorption isotherms of some cookies and corn snacks. *J. Food Eng.* **1997**, *31*, 85–93. [CrossRef]
32. Iglesias, H.A.; Chirife, J. Isosteric heats of water vapor sorption on dehydrated foods: I. Analysis of the differential heat curves. *LWT Lebensm. Wiss. Technol.* **1976**, *9*, 116–122.
33. Serris, G.S.; Biliaderis, C.G. Degradation kinetics of beetroot pigment encapsulated in polymeric matrices. *J. Sci. Food Agric.* **2001**, *81*, 691–700. [CrossRef]
34. Berg, J.C. The role of surfactants—The link between interfacial properties and absorbency. In *Absorbent Technology*, 1st ed.; Chatterjee, P.K., Gupta, B.S., Eds.; Elsevier: Amsterdam, The Netherlands, 2002; pp. 171–186, ISBN 0-444-50000-6.
35. Mark, R.E.; Habeger, C.C.; Borch, J.; Lyne, M.B. (Eds.) *Handbook of Physical Testing of Paper*, 2nd ed.; Marcel Dekker: New Yok, NY, USA, 2002; pp. 951–985. ISBN 0-8247-0498-3.
36. Ciesielskia, P.N.; Wagner, R.; Bharadwaj, V.S.; Jason Killgore, J.; Mittal, A.; Beckham, G.T.; Decker, S.R.; Himmel, M.E.; Crowley, M.F. Nanomechanics of cellulose deformation reveal molecular defects that facilitate natural deconstruction. *Proc. Natl. Acad. Sci. USA* **2019**, *116*, 9825–9830. [CrossRef]
37. Chatterjee, P.K.; Gupta, B.S. Measurement techniques for absorbent materials and products—Surface energetic of fibers. In *Absorbent Technology*; Chatterjee, P.K., Gupta, B.S., Eds.; Elsevier: Amsterdam, The Netherlands, 2002; pp. 395–397, ISBN 0-444-50000-6.
38. Hubbe, M.A.; Gardner, D.J.; Shen, W. Contact angles and Wettability of Cellulosic Surfaces A Review of Proposed Mechanisms and Test Strategies. *BioResources* **2015**, *10*, 8657–8749. [CrossRef]
39. Askling, C.; Wagberg, L. Effects of the process conditions during dry-defibration on the properties of cellulosic networks. *J. Mater. Sci.* **1998**, *33*, 2005–2012. [CrossRef]
40. Rebuzzi, F.; Evtuguin, D.V. Effect of glucuronoxylan on the hornification of *Eucalyptus globulus* bleached pulps. *Macromol. Symp.* **2005**, *232*, 121–128. [CrossRef]
41. Gross, J.R. The Evolution of Absorbent Materials. *Stud. Polym. Sci.* **1990**, *8*, 3–22. [CrossRef]
42. Pinto, P.C.; Evtuguin, D.V.; Pascoal Neto, C. Structure of hardwood glucuronoxylans: Modifications and impact on pulp retention during wood kraft pulping. *Carbohydr. Polym.* **2005**, *60*, 489–497. [CrossRef]
43. Liukkonen, A. Contact Angle of Water on Paper Components: Sessile Drops versusEnvironmental Scanning Electron Microscope Measurements. *Scanning* **1997**, *19*, 411–415. [CrossRef]
44. Koljonen, K.; Stenius, P. Surface characterisation of single fibres from mechanical pulps by contact angle measurements. *Nordic Pulp Paper Res. J.* **2005**, *20*, 107–114. [CrossRef]
45. Sousa, C.T.; Evtuguin, D.V.; Amaral, J.L. Hardwood kraft pulp structural features affecting refinability. *Holzforschung* **2017**, *71*, 619–624. [CrossRef]